Exploring Solar Dynamics: Magnetic Field and Differential Rotation Measurements

Yin Qiqin 211870080
School of Physics, Nanjing University
211870080@smail.nju.edu.cn

November 25, 2023

Abstract

This experimental study delves into the intricacies of solar dynamics through the simultaneous investigation of solar magnetic fields and differential rotation. We present a comprehensive review of the measurements of the solar magnetic field, tracing its roots in quantum mechanics to the challenges associated with determining the transverse field. We also discuss advanced methodologies for determining both the magnitude and orientation of the solar transverse magnetic field. Utilizing sunspots as "tracers", we establish a comprehensive relationship between latitude and rotation period, thereby highlighting the characteristics of solar differential rotation. In our measurement of the rotation period, we emphasize advanced statistical methods such as least squares fitting and curve fitting to ensure the precision and credibility of our results. Through meticulous analysis of synoptic data and the application of rigorous data analysis techniques, we aim to make a significant contribution to the broader understanding of solar physics. Our findings not only deepen our knowledge of solar dynamics but also pave the way for future research in this fascinating field.

1 Introduction

The Sun, as the central and most influential body in our solar system, exhibits a complex interplay of dynamic processes that profoundly impact the surrounding space environment. Two fundamental aspects of solar behavior, namely the solar magnetic field and the differential rotation of the Sun, play pivotal roles in shaping solar activity and influencing space weather phenomena. The basic concepts and properties of the solar magnetic field and the solar rotation are to be introduced in this part.

1.1 The solar magnetic field

The magnetic field of the Sun governs the formation of sunspots, solar flares, and coronal mass ejections, all of which contribute to the Sun's magnetic dynamics. The measurement and characterization of the solar magnetic field provide critical insights into the underlying processes that fuel solar phenomena and, by extension, affect the Earth and the broader heliosphere.

Generated by the motion of conductive plasma inside the Sun[Pid83], the solar magnetic field is a key driver of solar activity. This motion is created through convection. A localized magnetic field exerts a force on the plasma, effectively increasing the pressure without a comparable gain in density. As a result, the magnetized region rises relative to the remainder of the plasma, until it reaches the star's photosphere.

The solar magnetic field varies across the surface of the Sun. Its polar field is 1–2 gauss (0.0001–0.0002 T), whereas the field is typically 3,000 gauss (0.3 T) in sunspots and 10–100 gauss (0.001–0.01 T) in solar prominences. The magnetic field varies in time and location. The quasi-periodic 11-year solar cycle is the most prominent variation in which the number and size of sunspots waxes and wanes. During this dormancy, the sunspots activity is at maximum, and, as a result, massive ejection of high energy plasma into the solar corona and interplanetary space takes place.

The solar magnetic field is a three-dimensional vector field, meaning it has three components in space: one along the line of sight (radial component) and two perpendicular to it (transverse

components). The transverse components are typically further divided into two orthogonal directions, often referred to as the radial and azimuthal (or tangential) components. The transverse magnetic field is of particular interest because it provides insights into the structure and dynamics of the Sun's magnetic field. The study of transverse magnetic fields is crucial for understanding processes such as the formation of sunspots, the emergence of magnetic flux tubes, and the generation of solar flares and other solar activities.

1.2 The differential rotation of the Sun

Solar rotation varies with latitude. The Sun is not a solid body, but is composed of a gaseous plasma. Different latitudes rotate at different periods[Zel15]. The source of this differential rotation is an area of current research in solar astronomy. This differential rotation is argued to be caused by convective motion due to heat transport and the Coriolis force due to the Sun's rotation. The rate of surface rotation is observed to be the fastest at the equator (latitude $\varphi = 0°$) and to decrease as latitude increases. The solar rotation period is about 25.05 days at the equator and 34.4 days at the poles[Ste90].

The equatorial rotation period is not typically used, but instead we often uses the definition of a Carrington rotation: a synodic rotation period of 27.2753 days or a sidereal period of 25.38 days. This chosen period roughly corresponds to the prograde rotation at a latitude of 26° north or south, which is consistent with the typical latitude of sunspots and corresponding periodic solar activity.

The differential rotation rate is usually described by the equation[Bec00]:

$$\omega = A + B\ \sin^2(\varphi) + C\ \sin^4(\varphi)$$

where ω is the angular velocity in degrees per day, φ is the solar latitude, A is angular velocity at the equator, and B, C are constants controlling the decrease in velocity with increasing latitude. The values of A, B, and C differ depending on the techniques used to make the measurement, as well as the time period studied. A current set of accepted average values[SU90] is:

$$A = 14.713 \pm 0.0491°/day$$

$$B = -2.396 \pm 0.188°/day$$

$$C = -1.787 \pm 0.253°/day$$

With Wolfram Mathematica, we can plot solar rotation period as a function of latitude:

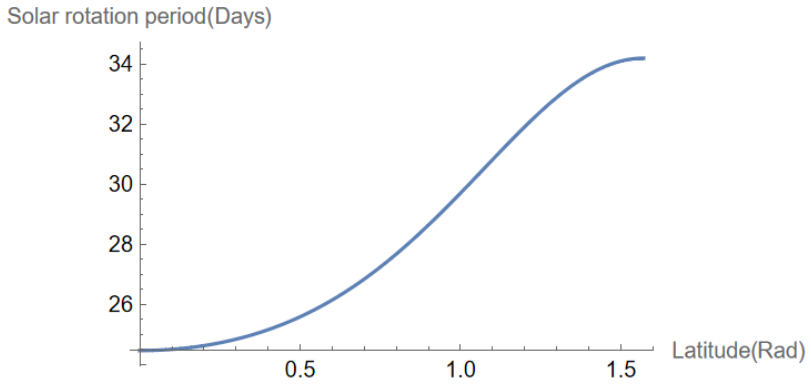

Figure 1: Solar Rotation Period Varies with Latitude

The Sun's rotation is counterclockwise, viewed from above the Sun's North Pole. When viewed from the Earth, sunspots are seen to move from left to right across the Sun's face. In Stonyhurst heliographic coordinates, the left side of the Sun's face is called East, and the right side of the Sun's face is called West. Therefore, sunspots are said to move across the Sun's face from east to west.

1.3 Objective of the Study

This experiment aims to deepen our understanding of the solar magnetic field and differential rotation by investigating into typical measurement techniques and analyzing the set of magnetic Field synoptic data.

Through searching in detail and meticulous data analysis, we seek to summarize a reliable method to measure the transverse magnetic field of the Sun unravel and quantify the differential rotation across latitudes. By doing so, we aspire to contribute to the broader body of knowledge in solar physics and enhance our ability to comprehend and predict solar activity.

2 Measurement of the solar transverse magnetic field

2.1 General idea

The magnetic field of the Sun can be measured by means of the Zeeman effect. Normally the atoms in a star's atmosphere will absorb certain frequencies of energy in the electromagnetic spectrum, producing characteristic dark absorption lines in the spectrum. When the atoms are within a magnetic field, however, these lines become split into multiple, closely spaced lines. The energy also becomes polarized with an orientation that depends on orientation of the magnetic field. Thus the strength and direction of the Sun's magnetic field can be determined by precise examination of the Zeeman effect lines[Wad04]. With the evolution of applying Zeeman effect to measure the solar magnetic field, more sophisticated and accurate techniques have been developed.

2.2 A brief introduction to Zeeman effect

The Zeeman effect is the effect of splitting of a spectral line into several components in the presence of a static magnetic field. The transitions between different components have, in general, different intensities, with some being entirely forbidden (in the dipole approximation), as governed by the selection rules.

Under the framework of quantum mechanics, we can demonstrate the Zeeman effect in the following case of a single atom. The total Hamiltonian of an atom in a magnetic field is[GS18]

$$H = H_0 + V_{\mathrm{M}},$$

where H_0 is the unperturbed Hamiltonian of the atom, and V_{M} is the perturbation due to the magnetic field: $V_{\mathrm{M}} = -\vec{\mu} \cdot \vec{B}$, where $\vec{\mu}$ is the magnetic moment of the atom.

The magnetic moment consists of the electronic and nuclear parts; however, the latter is many orders of magnitude smaller and will be neglected here. Therefore,

$$\vec{\mu} \approx -\frac{\mu_{\mathrm{B}} g \vec{J}}{\hbar},$$

where μ_{B} is the Bohr magneton, $\vec{J}$ is the total electronic angular momentum, and g is the Landé g-factor. As the total angular momentum assumes discrete values through the application of the ladder operator method, the term V_{M} delineates the nature of energy level splitting, specifically alleviating the degeneracy of energy levels. Hence, the relationship between the Zeeman splitting and external magnetic field could be written as:

$$\Delta E = \mu_{\mathrm{B}} g_J B_{\mathrm{ext}},$$

where the Landé g-factor g_J can be solved by implementing the angular momentum coupling. Consequently, the information of the Zeeman splitting in the solar spectra could reveal the magnitude of external magnetic field.

The different components of the split spectral lines correspond to different polarizations of light. The polarizations are classified as π (parallel to the magnetic field) and σ (perpendicular to the magnetic field). The π components have no frequency shift, while the σ components are shifted in frequency.

Since the distance between the Zeeman sub-levels is a function of magnetic field strength, this effect can be used to measure magnetic field strength. George Ellery Hale was the first to notice the Zeeman

effect in the solar spectra, indicating the existence of strong magnetic fields in sunspots. Such fields can be quite high, on the order of 0.1 tesla or higher. Today, the Zeeman effect is used to produce magnetograms showing the variation of magnetic field on the Sun.

2.3 Challenges of determining the transverse field

While significant strides have been made in measuring the solar magnetic field, determining its transverse component poses unique challenges.

One of the fundamental challenges arises from the observational geometry when studying the Sun from Earth. The line of sight is predominantly radial, making the Zeeman effect, which measures the longitudinal component, more readily observable. However, the transverse component, being perpendicular to the line of sight, where exists a 180° ambiguity[Hal08], requires specialized techniques and instruments to detect and measure accurately.

The signals associated with the transverse component are inherently weaker compared to the Zeeman splitting observed for the longitudinal component. This weaker signal, combined with the ambiguity in interpreting polarization signals, demands more sensitive instruments and sophisticated data analysis methods. The subtlety of transverse signals introduces an additional layer of complexity in accurately determining their strength and orientation. As a result, overcoming these challenges requires a combination of advancements in observational technologies, high spatial and temporal resolution instruments, and sophisticated data analysis techniques, which means that it is necessary to go beyond the somehow simple method using Zeeman effect.

2.4 The Milne-Eddington inversion

The Milne-Eddington inversion is a sophisticated technique used to infer the magnetic field properties, including the strength and orientation of the transverse component, by analyzing the polarization signals observed in spectral lines. This method assumes a simple model for the solar atmosphere, making it computationally efficient and suitable for analyzing large datasets. Grounded in radiative transfer theory, this method provides a more rigorous framework for analyzing spectropolarimetric data and extracting vital information about the strength and orientation of the transverse magnetic field.

The foundation of the Milne-Eddington inversion lies in the radiative transfer equation, which governs the propagation of light through a medium. It takes this form:

$$I(\lambda,\mu) = I_0(\lambda)e^{-\tau(\lambda,\mu)} + \int_0^{\tau(\lambda,\mu)} S(\lambda,\mu,\tau')e^{-\tau'}\,d\tau',$$

where I is the emergent intensity, λ is the wavelength, μ is the cosine of the angle with the solar normal, τ is the optical depth, and S is the source function[Bom16].

For polarized light, the Stokes parameters (I, Q, U, V) encapsulate the polarization state. In the context of a spectral line, the linear polarization parameters (Q, U) play a pivotal role in characterizing the transverse magnetic field.

To simplify the above equation of radiactive transfer, an approximation, called the Eddington approximation, has been applied. This approximation, also known as Milne-Eddington model, assumes a simplified one-dimensional plane-parallel atmosphere. This model approximates the source function as linear in optical depth:

$$I_\nu(\mu, z) = a(z) + \mu b(z),$$

where where z is the normal direction to the slab-like medium and μ is still the cosine of the angle with the solar normal, facilitating a computationally efficient solution to the radiative transfer equation. While this simplification is a strength in terms of computational efficiency, it acknowledges the complexity of the actual solar atmosphere.

The heart of the Milne-Eddington inversion involves an iterative process where observed Stokes profiles are compared with synthetic profiles generated by the model. Adjustments to parameters, including the magnetic field strength and orientation, are made until the synthetic profiles closely match the observed ones. This iterative inversion process unveils the underlying properties of the solar atmosphere, particularly the transverse magnetic field.

Since the Stokes parameters are acquired in the experiment, it is possible to solve the strength and direction of solar transverse magnetic field. The transverse magnetic field contributes significantly to the Q and U Stokes parameters. These parameters, representing linear polarization, offer insights into the transverse magnetic field strength and orientation. The degree of polarization (P) and the azimuth angle (ϕ) of the transverse magnetic field can be derived from Q and U using the following formulas:

$$P = \sqrt{Q^2 + U^2},$$

$$\phi = \frac{1}{2} \arctan \frac{U}{Q}.$$

These calculations provide a quantitative representation of the transverse magnetic field, allowing astronomers to discern the intricate dynamics of solar magnetism. Finally, the strength and orientation of the transverse magnetic field (B_{trans}) can be calculated from P and ϕ, as the magnitude of (B_{trans}) is proportional to the degree of polarization (P) and the azimuth angle (ϕ) reveals the direction of the magnetic field in the plane perpendicular to the line of sight.

While the Milne-Eddington inversion is a powerful tool, it is not without challenges. The method assumes a one-dimensional atmosphere and may not fully capture the complexities of the solar environment. Ongoing research focuses on refining inversion techniques by incorporating multi-line and multi-atom information to address these challenges.

In conclusion, the Milne-Eddington inversion stands as a robust methodology for determining the transverse component of the solar magnetic field. As computational capabilities advance and observational data become more sophisticated, inversion techniques play a pivotal role in advancing our understanding of the dynamic solar atmosphere. The transverse magnetic field, revealed through such methods, unlocks valuable insights into the complex interplay of magnetic forces shaping the Sun's behavior.

3 Solar differential rotation

The determination of solar rotation constants involves tracking the motion of distinct features, often referred to as "tracers", on the solar surface. This section focuses on calculating the solar rotation period at various latitudes by monitoring the positional changes of sunspots, a widely utilized tracer, over a span of several days. To enhance the accuracy of our findings and gain a deeper insight into the characteristics of solar rotation, statistical techniques are employed. The results are then rigorously analyzed, including a comparison with the accepted value associated with solar differential rotation, allowing for a thorough examination of experimental errors. The concluding segment of this section delves into discussions on potential enhancements for measuring solar rotation, fostering a comprehensive exploration of methods for refining our understanding of this fundamental solar property.

3.1 Data source and description for solar rotation calculation

The data presented in this report were sourced from SolarMonitor [GMW02], a website hosted by the Solar Physics Group at Trinity College Dublin and the Dublin Institute for Advanced Studies. These pages provide both near-real-time and archived information on active regions and solar activity.

To ascertain the solar rotation period at a specific latitude, sunspots serve as pertinent tracers. Through the meticulous recording of a sunspot's positional changes over a defined temporal span, the rotational period can be deduced at various latitudes. It is imperative to acknowledge, however, that the determination of the geometric center of a sunspot poses challenges due to its vigorous activities on the Sun's photosphere. Additionally, fluctuations in the temporal strength of solar activities may introduce variability into the derived results.

Taking into account the aforementioned considerations, the positional changes of four sunspot events, documented from late July to early August of 2022, were utilized to compute solar differential rotation. These selected sunspot events, situated at distinct latitudes and in close temporal proximity, were sourced from SolarMonitor.org. The website's pages offer time intervals of nearly one day, with errors in the order of seconds, and furnish information on the latitude, longitude, and NOAA number of each sunspot event[Tho06]. The provision of NOAA numbers enhances the ease of tracking sunspots during the solar rotation process.

Specifically, the information of four sunspots at different latitudes, which approximately uniformly distributed at latitudes of S08, S15, S19, S25, is recorded in the following tables.

In this experiment, the dataset comprises positional and temporal information pertaining to four distinct sunspot events. Each sunspot is uniquely identified by its NOAA number, with their respective latitudinal coordinates denoted in a structured format: (13062, S25), (13065, S19), (13068, S15), and (13059, S08). Here, the numerical component represents the NOAA number assigned to each sunspot event, while the letter "S" prefacing the latitude designates its southern location. Deliberate selection of these latitudes ensures a uniform interval spacing, contributing to the strategic distribution of observational data. The rigorous arrangement of these parameters enables a meticulous examination of the solar phenomena under investigation.

The data of the four events and the figures of the sunspots' positions at different times are respectively listed as follows.

Date	**Longitude(Deg)**	**Latitude(Deg)**
2022.7.22	E34	S25
2022.7.23	E22	S26
2022.7.24	E09	S25
2022.7.25	W04	S25
2022.7.26	W17	S25
2022.7.27	W30	S26

Table 1: Position Change Over Sunspot (NOAA Number: 13062)

Date	**Longitude(Deg)**	**Latitude(Deg)**
2022.7.22	E01	S19
2022.7.23	W13	S19
2022.7.24	W26	S19
2022.7.25	W40	S19
2022.7.26	W54	S19
2022.7.27	W65	S20

Table 2: Position Change Over Sunspot (NOAA Number: 13065)

Date	**Longitude(Deg)**	**Latitude(Deg)**
2022.7.29	E44	S16
2022.7.30	E31	S15
2022.7.31	E16	S15
2022.8.1	E02	S15
2022.8.2	W12	S15
2022.8.3	W26	S15

Table 3: Position Change Over Sunspot (NOAA Number: 13068)

Date	Longitude(Deg)	Latitude(Deg)
2022.7.19	E15	S10
2022.7.20	E01	S07
2022.7.21	W14	S08
2022.7.22	W28	S08
2022.7.23	W42	S08
2022.7.24	W56	S08

Table 4: Position Change Over Sunspot (NOAA Number: 13059)

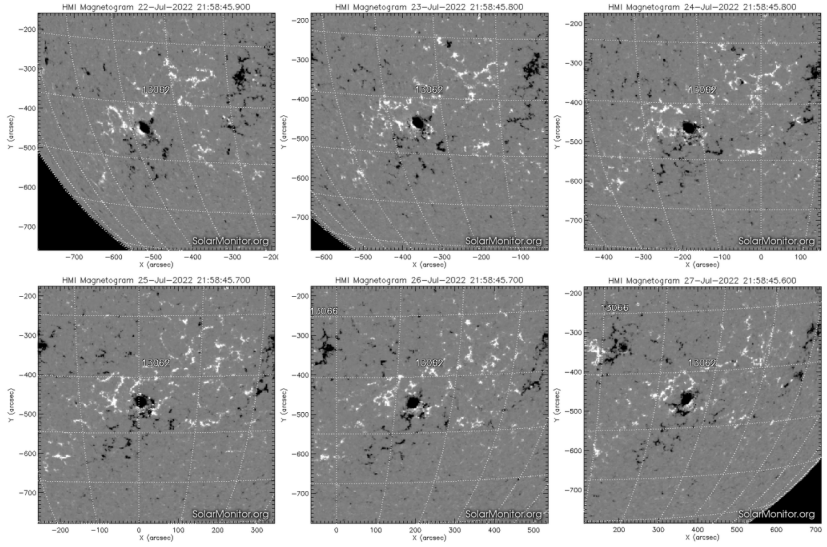

Figure 2: Position Change Over Sunspot 13062 from July 22 to July 27

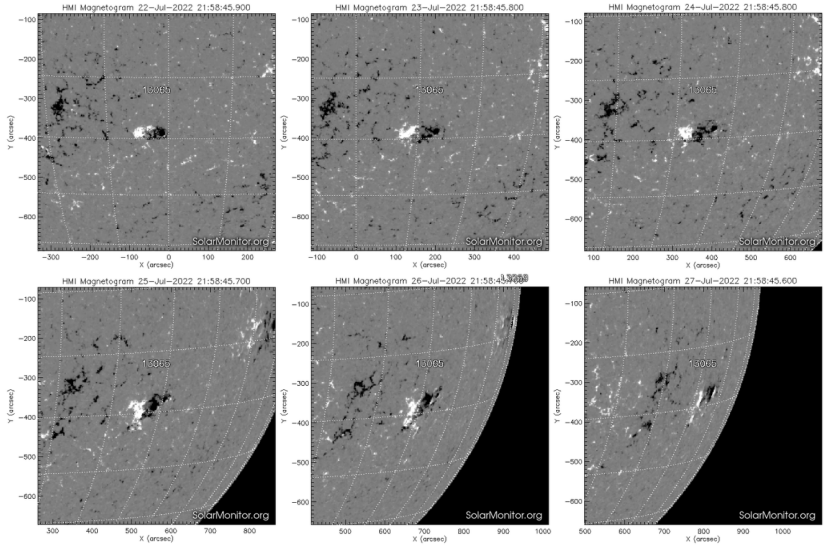

Figure 3: Position Change Over Sunspot 13065 from July 22 to July 27

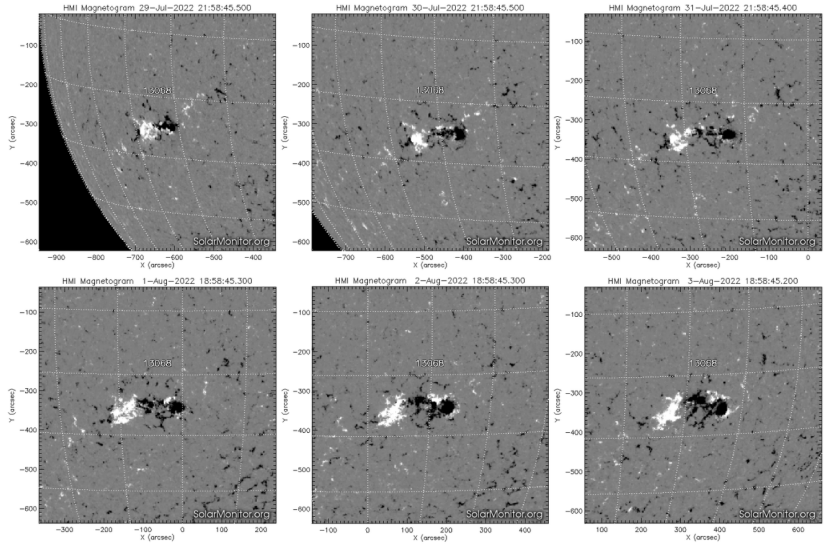

Figure 4: Position Change Over Sunspot 13068 from July 29 to Aug 3

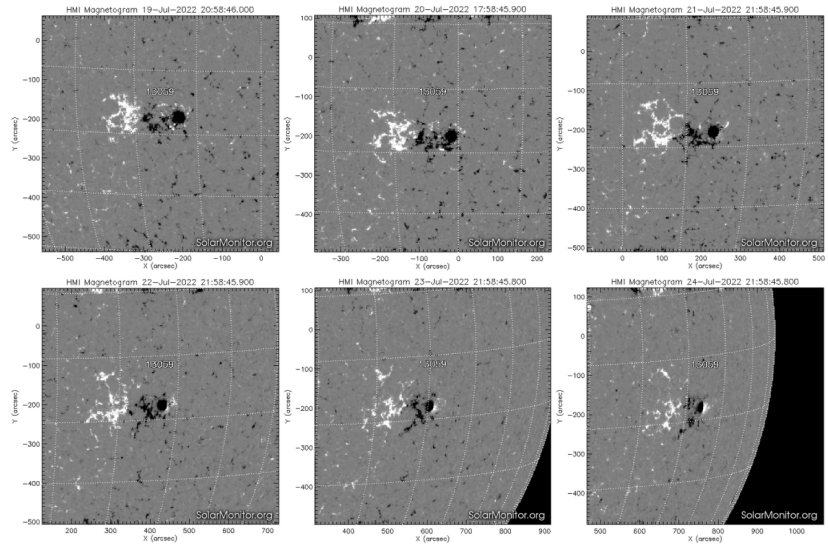

Figure 5: Position Change Over Sunspot 13059 from July 19 to July 24

3.2 Determination of rotation period

The observational data suggests that the latitudinal position of each sunspot event remains relatively constant as the Sun rotates. This consistency allows for the determination of the Sun's rotation periods at different latitudes, derived from the variation in longitudinal values over a span of six consecutive days. To enhance the precision of these determinations, a commonly utilized statistical method known as least squares fitting is employed. This technique optimizes the accuracy of the rotation period measurements by minimizing the sum of the squares of the residuals.

The least squares fitting is implemented using the "Fit" function in Wolfram Mathematica. This function allows us to derive the slope of each fitting curve from the raw data of the four events observed in our experiment. It's important to note that the time interval between consecutive observations is approximately one day, with an error margin of only a few seconds, which falls within the acceptable accuracy range of our experiment. Therefore, the unit of the horizontal axis is designated as "days". Given that the critical data point in this experiment is the slope, which is proportional to the angular velocity, the intercept of the curve provides minimal relevant information. Consequently, we have the

liberty to set the time of the earliest event as 1 on the horizontal axis. This approach simplifies the data representation without compromising the integrity of the experiment.

The results of the fitting process are graphically represented in the subsequent plots. In this visualization, the raw data points are denoted by red markers, while the fitted lines, derived from our mathematical functions, are also included for comprehensive analysis. This dual representation facilitates a clear comparison between the observed data and our fitting model.

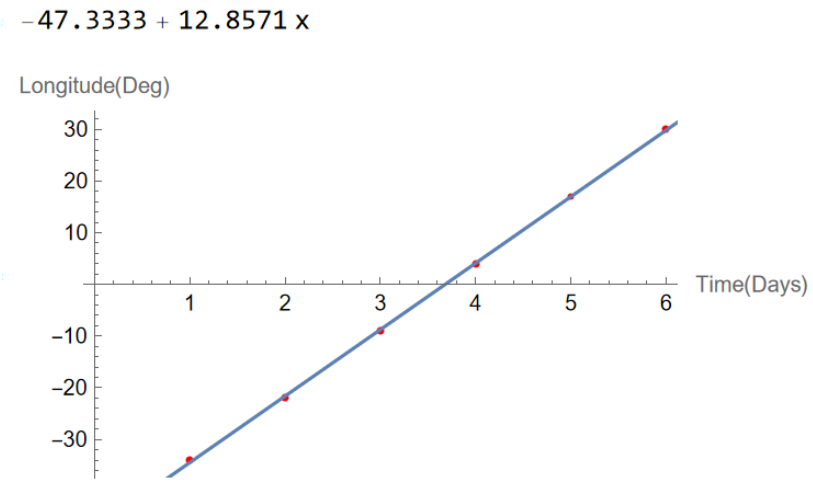

Figure 6: Least Squares Fitting of 13062

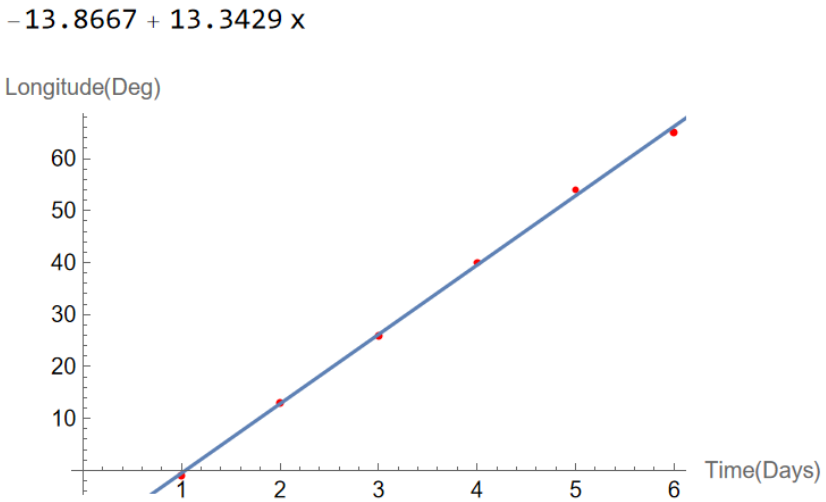

Figure 7: Least Squares Fitting of 13065

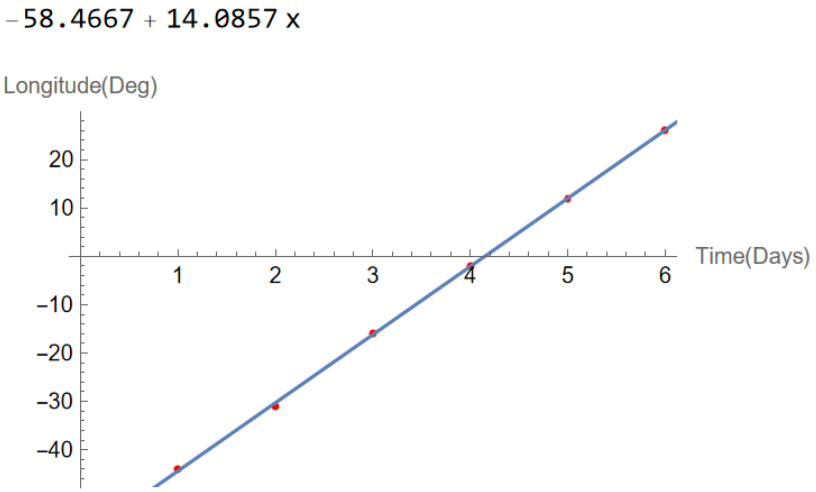

Figure 8: Least Squares Fitting of 13068

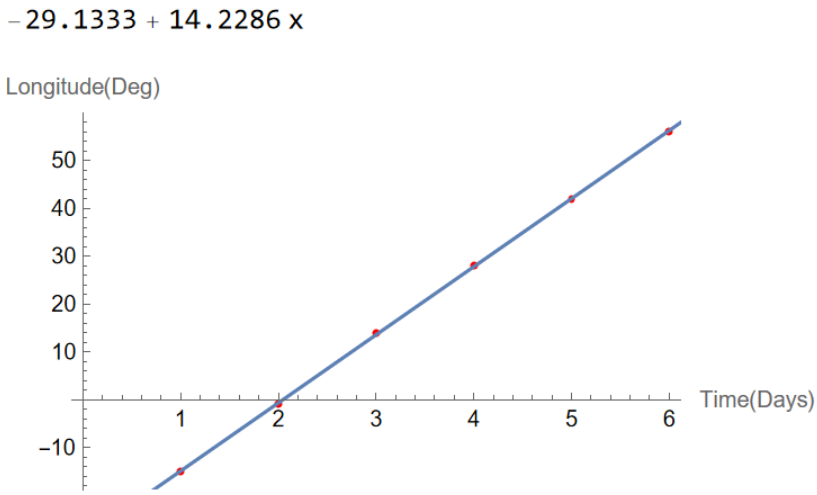

Figure 9: Least Squares Fitting of 13059

Finally, since the slopes are known, the periods of rotation at four different latitudes can be calculated by this equation:

$$T = \frac{360^\circ}{k},$$

where T is the period of rotation and k is the slope. The results are listed in the table below.

NOAA Number	Average Latitude(Deg)	Rotation Period(Days)
13062	S25.33	28.00
13065	S19.17	26.98
13068	S15.17	25.56
13059	S08.17	25.30

Table 5: Rotation Periods at Four Different latitudes

3.3 Result and analysis

Having obtained the rotation period at four distinct latitudes, we observe a trend of increasing rotation period with increasing latitude. This implies a decrease in rotational speed as we move away from the

Sun's equator. To illustrate this trend, we have plotted the data points from Table 5 in a figure where the horizontal axis represents latitude and the vertical axis represents the rotation period.

To establish a comprehensive relationship between latitude and rotation period, we have employed a curve fitting method. This method is based on the "FindFit" function in Wolfram Mathematica, a widely used tool for finding the globally optimal fit subject to given parameter constraints. This function requires an expression of the desired fitting function form.

To evaluate the precision of our experiment, we have compared the fitted curve with the accepted average values of the solar rotation period as a function of latitude, as presented in the introduction. This comparison necessitates that the expression of the fitting function aligns with the form:

$$T = \frac{360^\circ}{A + B\sin^2(\varphi) + C\sin^4(\varphi)},$$

where T represents the rotation period, ϕ is the absolute value of latitude and A, B, C are three fitting parameters. The following figure exhibit the data points, the fitted curve along with the curve with accepted values of A, B and C in section 1.2.

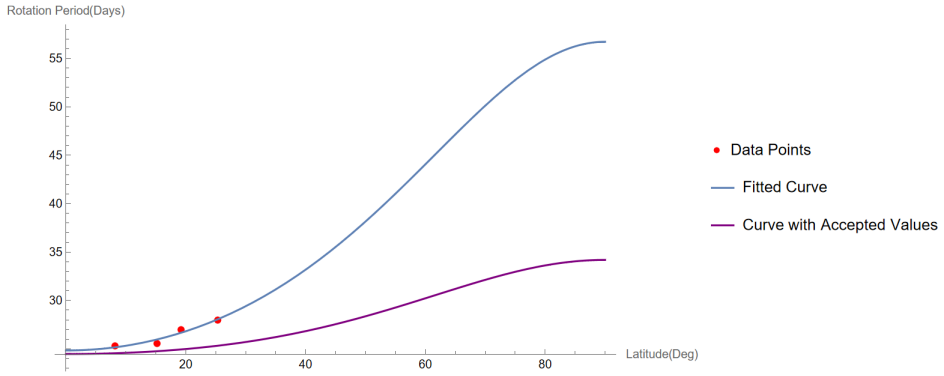

Figure 10: Fitted Results Showing the Relation of Rotation Period and Latitude

The fitting process above gives out the optimized value of A, B and C:

$$A_{\text{fit}} = 14.494 \pm 0.0491^\circ/day,$$

$$B_{\text{fit}} = -9.287 \pm 0.188^\circ/day,$$

$$C_{\text{fit}} = -1.140 \pm 0.253^\circ/day.$$

Upon comparison, we discover that the period of rotation at the equator of the Sun in the fitted result almost coincide with the accepted value, which can be determined by:

$$T_0 = \frac{360^\circ}{A},$$

where the index 0 denotes the zero value of latitude i.e. the rotation period at equator.Therefore, it is calculated that:

$$T_{0\text{fit}} = \frac{360^\circ}{A_{\text{fit}}} = 24.838 days,$$

$$T_{0\text{acp}} = \frac{360^\circ}{A_{\text{acp}}} = 24.468 days,$$

where the index fit and acp represent the fitted and the accepted values respectively.

The above calculation along with Figure 10 both reveals that the period of rotation at equator in our experiment has good precision compared with the accepted value, with an relative error that:

$$\Delta = \frac{|T_{0\text{fit}} - T_{0\text{acp}}|}{T_{0\text{acp}}} = 1.512\%.$$

However, it is observed that as the latitude increases, the associated error also tends to increase. This can be partly attributed to the fact that our data is primarily distributed at latitudes lower than 30°. Observationally, sunspots are typically found at latitudes below this threshold, resulting in a lack of constraints on the fitting parameters at higher latitudes.

Our analysis of these trends and errors suggests that the observation of rare sunspot events at higher latitudes could potentially provide additional constraints on the results. This, in turn, could enhance the precision of this experiment, offering a more accurate representation of solar activity across a broader range of latitudes. This insight underscores the importance of comprehensive data collection in ensuring the accuracy and reliability of our experimental findings.

With further consideration, to precisely determine the rotation period, if the "tracer" method is still applied, it is necessary to trace some solar events that happen more frequently at higher latitudes. Therefore, this will give more constraints on our model of angular velocity at different latitudes on the solar surface. Alternatively, some advanced techniques based on modern Physics can rescue this.One possible alternative is to use the Doppler shift of the solar spectral lines to infer the rotation speed of the solar photosphere at different latitudes. This method relies on the fact that the solar material at the limb (the edge of the sun) has a radial velocity component that causes a shift in the wavelength of the observed light. By measuring the Doppler shift at different positions on the solar disk, you can calculate the angular velocity of the sun as a function of latitude. This method does not depend on the presence of sunspots, and it can be applied to any spectral feature that is visible in the solar spectrum.

4 Conclusions

Our experimental study meticulously explores the complexities of solar dynamics, focusing on the concurrent examination of solar magnetic fields and differential rotation. Our report underscores the difficulties encountered in quantifying the transverse component of the solar magnetic field, thereby accentuating the necessity for specialized methodologies and instrumentation for its precise detection and measurement.

We have innovatively employed a curve fitting technique to delineate a comprehensive correlation between latitude and rotation period, thereby augmenting our comprehension of solar activity across an expanded latitude spectrum. This investigation significantly enriches our understanding of solar physics, offering valuable insights into the characteristics of the solar atmosphere and bolstering our capacity to interpret and forecast solar phenomena.

References

[Bec00] John G Beck. A comparison of differential rotation measurements–(invited review). *Solar physics*, 191(1):47–70, 2000.

[Bom16] Véronique Bommier. Milne-eddington inversion for unresolved magnetic structures in the quiet sun photosphere. *Journal of Geophysical Research: Space Physics*, 121(6):5025–5040, 2016.

[GMW02] Peter T Gallagher, Y-J Moon, and Haimin Wang. Active-region monitoring and flare forecasting–i. data processing and first results. *Solar Physics*, 209:171–183, 2002.

[GS18] David J Griffiths and Darrell F Schroeter. *Introduction to quantum mechanics*. Cambridge university press, 2018.

[Hal08] George E Hale. On the probable existence of a magnetic field in sun-spots. *Astrophysical Journal, vol. 28, p. 315*, 28:315, 1908.

[Pid83] JH Piddington. On the origin and structure of stellar magnetic fields. *Astrophysics and Space Science*, 90:217–230, 1983.

[Ste90] JO Stenflo. Time invariance of the sun's rotation rate. *Astronomy and Astrophysics (ISSN 0004-6361), vol. 233, no. 1, July 1990, p. 220-228.*, 233:220–228, 1990.

[SU90] Herschel B Snodgrass and Roger K Ulrich. Rotation of doppler features in the solar photosphere. *Astrophysical Journal, Part 1 (ISSN 0004-637X), vol. 351, March 1, 1990, p. 309-316.*, 351:309–316, 1990.

[Tho06] WT Thompson. Coordinate systems for solar image data. *Astronomy & Astrophysics*, 449(2):791–803, 2006.

[Wad04] Gregg A Wade. Stellar magnetic fields: the view from the ground and from space. *Proceedings of the International Astronomical Union*, 2004(IAUS224):235–243, 2004.

[Zel15] Holly Zell. Solar rotation varies by latitude, 2015.